

Free microparticles—An inducing mechanism of pre-firing in high pressure gas switches for fast linear transformer drivers

Xiaoang Li, Zehao Pei, Zhicheng Wu, Yuzhao Zhang, Xuandong Liu, Yongdong Li, and Qiaogen Zhang

Citation: [Review of Scientific Instruments](#) **89**, 035113 (2018); doi: 10.1063/1.5020727

View online: <https://doi.org/10.1063/1.5020727>

View Table of Contents: <http://aip.scitation.org/toc/rsi/89/3>

Published by the [American Institute of Physics](#)

Articles you may be interested in

[Exploring microwave resonant multi-point ignition using high-speed schlieren imaging](#)

[Review of Scientific Instruments](#) **89**, 034701 (2018); 10.1063/1.5009273

[Note: Additionally refined new possibilities of plasma probe diagnostics](#)

[Review of Scientific Instruments](#) **89**, 036102 (2018); 10.1063/1.5022236

[A portable liquid crystal-based polarized light system for the detection of organophosphorus nerve gas](#)

[Review of Scientific Instruments](#) **89**, 035001 (2018); 10.1063/1.5000860

[A compact nanosecond pulse generator for DBD tube characterization](#)

[Review of Scientific Instruments](#) **89**, 033505 (2018); 10.1063/1.5017564

[Experiments of a 100 kV-level pulse generator based on metal-oxide varistor](#)

[Review of Scientific Instruments](#) **89**, 034705 (2018); 10.1063/1.5012555

[An effective temperature compensation approach for ultrasonic hydrogen sensors](#)

[Review of Scientific Instruments](#) **89**, 035005 (2018); 10.1063/1.5017639



Scilight

Sharp, quick summaries **illuminating**
the latest physics research

Sign up for **FREE!**

AIP
Publishing

Free microparticles—An inducing mechanism of pre-firing in high pressure gas switches for fast linear transformer drivers

Xiaoang Li,^{1,a)} Zhehao Pei,¹ Zhicheng Wu,¹ Yuzhao Zhang,¹ Xuandong Liu,¹ Yongdong Li,² and Qiaogen Zhang¹

¹State Key Laboratory of Electrical Insulation and Power Equipment, School of Electrical Engineering, Institute of High Voltage Technology, Xi'an Jiaotong University, Xi'an 710049, China

²School of Electronics and Information Engineering, Institute of Electrical Science and Technology, Xi'an Jiaotong University, Xi'an 710049, China

(Received 26 December 2017; accepted 4 March 2018; published online 26 March 2018)

Microparticle initiated pre-firing of high pressure gas switches for fast linear transformer drivers (FLTDs) is experimentally and theoretically verified. First, a dual-electrode gas switch equipped with poly-methyl methacrylate baffles is used to capture and collect the microparticles. By analyzing the electrode surfaces and the collecting baffles by a laser scanning confocal microscope, microparticles ranging in size from tens of micrometers to over 100 μm are observed under the typical working conditions of FLTDs. The charging and movement of free microparticles in switch cavity are studied, and the strong DC electric field drives the microparticles to bounce off the electrode. Three different modes of free microparticle motion appear to be responsible for switch pre-firing. (i) Microparticles adhere to the electrode surface and act as a fixed protrusion which distorts the local electric field and initiates the breakdown in the gap. (ii) One particle escapes toward the opposite electrode and causes a near-electrode microdischarge, inducing the breakdown of the residual gap. (iii) Multiple moving microparticles are occasionally in cascade, leading to pre-firing. Finally, as experimental verification, repetitive discharges at ± 90 kV are conducted in a three-electrode field-distortion gas switch, with two 8 mm gaps and pressurized with nitrogen. An ultrasonic probe is employed to monitor the bounce signals. In pre-firing incidents, the bounce is detected shortly before the collapse of the voltage waveform, which demonstrates that free microparticles contribute significantly to the mechanism that induces pre-firing in FLTD gas switches. *Published by AIP Publishing.* <https://doi.org/10.1063/1.5020727>

I. INTRODUCTION

For output-power duplication, fast linear transformer drivers (FLTDs) use “multi-bricks” with low (LC)^{1/2} to discharge synchronously and have potential applications in Z-pinch systems, high-power lasers, x-ray radiography, etc.^{1–4} The circuit topologies of FLTDs are such that they require a large amount of gas switch, which means that the negative effects of pre-firing can be greatly intensified. Therefore, a fundamental requirement of gas switches for FLTDs is a low probability of pre-firing.^{5–8} Although many types of gas switches have been developed, the pre-fire probability for FLTDs is far from satisfactory.^{9–15} Analyzing and clarifying the inducing mechanisms of pre-fire is necessary for reducing the pre-fire probability of gas switches.

The results reported herein indicate that typical FLTD-discharge conditions generate microparticles in the switch cavity. The behavior of these microparticles under strong DC electric fields is examined in an FLTD gas switch, and their influence on breakdown voltage is estimated. In addition, how the behaviors of microparticles affect the pre-firing of FLTD gas switches is analyzed and the pre-fire inducing mechanisms are experimentally verified in a low-inductance three-electrode field-distortion gas switch.

II. EVIDENCE OF FREE MICROPARTICLES IN FLTD GAS SWITCHES

To study the size and distribution of microparticles generated in a switch cavity under typical FLTD working conditions (30 kA discharge current, 60 ns rise time, at ± 100 kV), a classical dual-electrode gas switch equipped with the poly-methyl methacrylate baffles reported in Ref. 16 is used, which allows us to capture and collect particles.¹⁶ Figure 1 shows several images of such microparticles from several different perspectives. Figure 1(a) shows a photograph of the electrode surface after repetitive discharges, which severely erode the electrode surface and create numerous etch pits in the center surrounded by a significant amount of erasable powder. The powder is thought to be formed by the condensation of the metal vapor generated in the electrode-erosion process. Figure 1(b) shows the local uneven morphology of the electrode surface, as imaged by a laser scanning confocal microscope (LSCM). The surface roughness R_z (i.e., maximum height of profile peaks) reaches 100 μm . Figure 1(c) shows the microparticles fixed to the electrode surface through the droplet ejection process. Note that most microparticles have a fairly regular shape. The ejected microparticles are tens of micrometers in size and are difficult to move. Figure 1(d) shows transmission electron microscopy (TEM) images of the surrounding powder. The powder ranges in diameter from tens to hundreds of nanometers. Figure 1(e) shows a LSCM

^{a)}Author to whom correspondence should be addressed: li_xiaoang@mail.xjtu.edu.cn

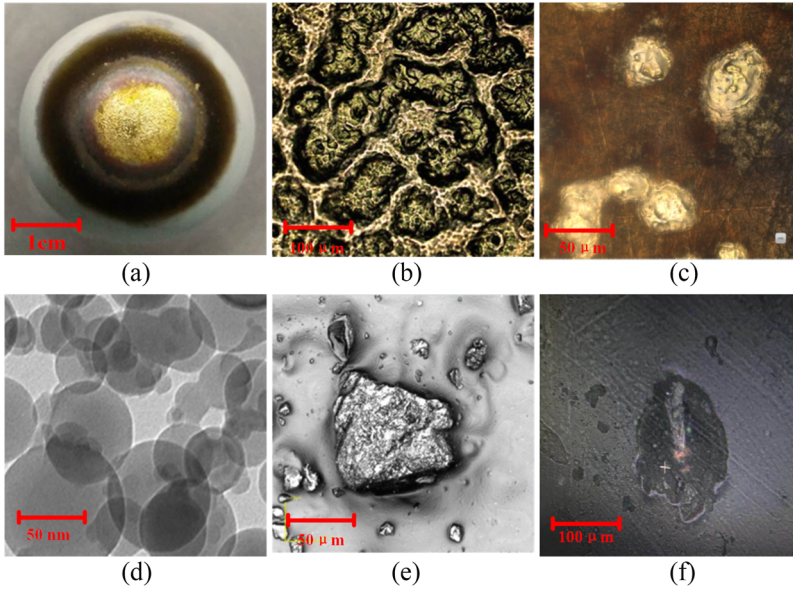


FIG. 1. Evidence of microparticles in switch cavity (30 kA with a 60 ns rise time, at ± 100 kV). (a) Macro morphology of the electrode, (b) local morphology of the central eroded part, (c) droplet ejection, (d) TEM image of powder, (e) particles gathered by the baffle, and (f) free microparticles in switch cavity.

image of the surface of the gathering baffle, which shows an irregularly shaped microparticle. The particle is thought to be formed from the solid material removed during the electrode erosion process. In an FLTD gas switch, a high-amplitude short-duration current pulse can create across the switch gap a thin spark channel with extremely high current density. This spark generates extremely strong forces at the spark-electrode interface and removes some of the electrode material before the phase change.^{16,17} In addition, several free microparticles appear at the bottom of the switch cavity, one of which is shown attached to transparent tape by the backlit photomicrograph in Fig. 1(f). The diameter of these free microparticles is $\sim 100 \mu\text{m}$.

Thus, particles are clearly generated in repetitive discharges, mainly by electrode erosion.^{18–20} The size of these particles varies, ranging from submicrometer powder particles to free micrometer-sized particles. These particles are subject to a DC electric field and can be charged and moved by electrostatic forces. Note that gas switches for FLTDs are generally compact to satisfy the low-inductance requirement and have relatively small gaps and high gas pressure, which results in strong electric fields, even exceeding 100 kV/cm, across the switch gap.^{13,14} In such conditions, free microparticles could be easily charged and would be subject to strong electrostatic forces, possibly sufficient to move free microparticles and thereby obviously decrease the insulation strength of the switch gap.^{21–25}

III. BEHAVIOR OF FREE METALLIC MICROPARTICLES

A. Charging and movement of free metallic microparticles

To simplify the analysis, we consider the metallic particles as spheres and express the charge q on these spheres as^{21,25}

$$q = \frac{1}{6} \pi^3 d^2 \varepsilon E_0, \quad (1)$$

where d is the particle diameter in meters, ε is the dielectric constant of the gas in the switch gap [$8.85 \times 10^{-12} \text{ C}^2/(\text{N m}^2)$], and E_0 is the DC electric field in kV/cm. The charged particle is subjected to the electrostatic force²¹

$$F_q = kqE_0, \quad (2)$$

where k is a correction factor due to the image charge when the particle is adjacent to the electrode ($k \approx 0.8$). Once the electrostatic force F_q overcomes the force G of gravity, the particle moves. Thus, the condition for the particle to move is

$$F_q \geq G. \quad (3)$$

The force G of gravity is

$$G = \frac{4}{3} \pi a^3 \rho g, \quad (4)$$

where ρ is the particle density and g is the acceleration due to gravity (9.8 m/s^2). Combining Eqs. (1)–(4) gives the critical electric field E_0 to make a particle move,

$$E_0 \geq 0.45 \sqrt{ag\rho/\varepsilon k}. \quad (5)$$

For a stainless-steel 100- μm -diameter spherical particle, $\rho = 7800 \text{ kg/m}^3$ and $E_0 = 2.3 \text{ kV/cm}$. However, because of the van der Waals force F_v exerted by the surface of the adjacent electrode on the particle, the particle can move only when $F_q > G + F_v$. Note that F_v is related to the contact area and cannot be ignored for small particles (with a low mass-area ratio). The critical electric field E_{jump} for a particle to jump is

$$E_{\text{jump}} = \beta \cdot E_0, \quad (6)$$

where β is a correction factor. A plate-plate gap equipped with an ultrasonic probe is used to experimentally study E_{jump} and then β is calculated by E_{jump}/E_0 . The results are shown in Fig. 2, where E_{jump} increases with the increase of particle size, while β shows an opposite trend. Besides, note that both the amplitude and time interval of the ultrasonic signals depend weakly on the applied voltage and strongly on the particle size.

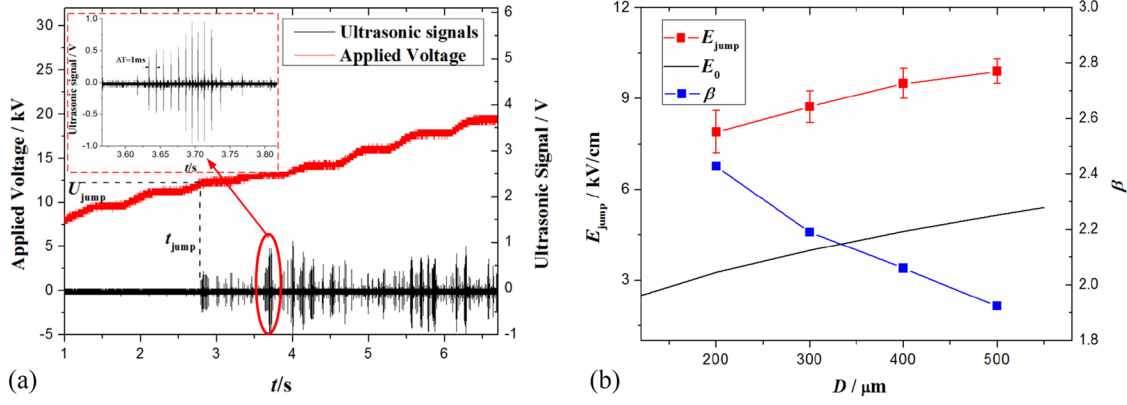


FIG. 2. Ultrasonic signals indicating particle bounce and E_{jump} . (a) Applied voltage and ultrasonic signals (500 μm) and (b) critical electric field E_{jump} and β .

According to the experimental results, $E_{\text{jump}} \approx 10 \text{ kV/cm}$ for particles hundreds of micrometers in diameter, which is much less than the common electric field across a switch gap in FLTDs. Thus, once free microparticles are generated during switch operation, for whatever reason (e.g., electrode erosion),¹⁶ the conditions for them to begin jumping are easily satisfied. This allows the particles to “bounce” off the electrode surface within the switch cavity, which may reduce the breakdown voltage and induce pre-firing.

B. Pre-fire-inducing mode

Free microparticles can alter the electric field enhancement factor and reduce the insulation strength of the gas gap. According to the state of the free microparticles and their location and number, the breakdown voltage of the gas gap may be lowered depending on the specific mode (see below) of microparticle motion.

1. Mode I

When a free microparticle lies on and becomes fixed to the electrode surface, it becomes a fixed protrusion and enhances the local electric field, resulting in a quasi-uniform background electric field on which is superimposed a local distortion, which can cause a partial discharge from the electrode surface and thereby induce breakdown across the entire gas gap, as depicted in Fig. 3.

The electric field distortion in mode I can be calculated using the Pederson model, following which the breakdown voltage of the gas gap can be estimated. First, the particle

is approximated by a hemisphere of the same height as the microparticle. The electric field at the apex of the hemisphere in the x direction is²⁶

$$E(x) = E_0[1 + 2(h/x)^3], \quad (7)$$

where E_0 is the background electric field in kV/cm and h is the radius of the hemisphere.

Next, considering the high pressure nitrogen gap and the quasi-uniform background electric field, an electron avalanche developing above the protrusion may easily lead to a breakdown across the gap.^{26–28} In this case, the threshold of the switch breakdown is determined by the streamer breakdown criterion (i.e., Shuman’s equation),²⁶

$$\int_0^l \bar{\alpha}(x) dx = k, \quad (8)$$

where $\bar{\alpha}(x)$ is the effective coefficient of ionization along the x direction in the gap and k is a constant. For nitrogen, $k = 5$ and the effective coefficient α of ionization depends on the electric field and pressure as follows:²⁷

$$\alpha_{N_2}(E, P) = 66P \cdot \exp\left(\frac{-2.15}{E/P}\right), \quad (9)$$

where E is the electric field in kV/cm and P is the pressure in kPa. Therefore, according to Shuman’s equation, the criterion for breakdown across the gas gap is

$$k_{N_2} = \int_{R_z}^l 66P \cdot \exp\left(\frac{-2.15P}{\frac{U}{7f} \cdot [1 + 2(R_z/x)^3]}\right) dx = 5. \quad (10)$$

Considering a single 15 mm plate-plate gap and ignoring edge effects, Fig. 4 shows the U_b versus P curve (where U_b is the breakdown voltage and P is the pressure) for the gap as calculated by Eq. (10). With increasing particle size, U_b decreases. In addition, U_b becomes more sensitive to the microparticle size at higher pressure. For example, a 180- μm -diameter particle causes a 12% reduction in U_b at 0.1 MPa but a 23% reduction at 0.6 MPa. According to aforementioned results, microparticles generated during the repetitive operation of FLTD gas switches range from tens of micrometers to over 100 μm , resulting in a limited decrease of insulation strength of switch gap. Thus, pre-firing can often be

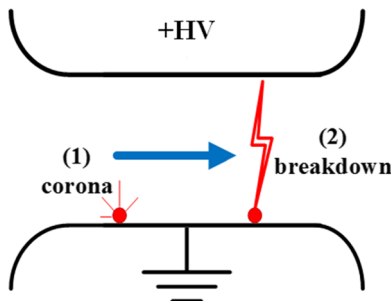


FIG. 3. Mode I: local-field distortion and partial discharge.

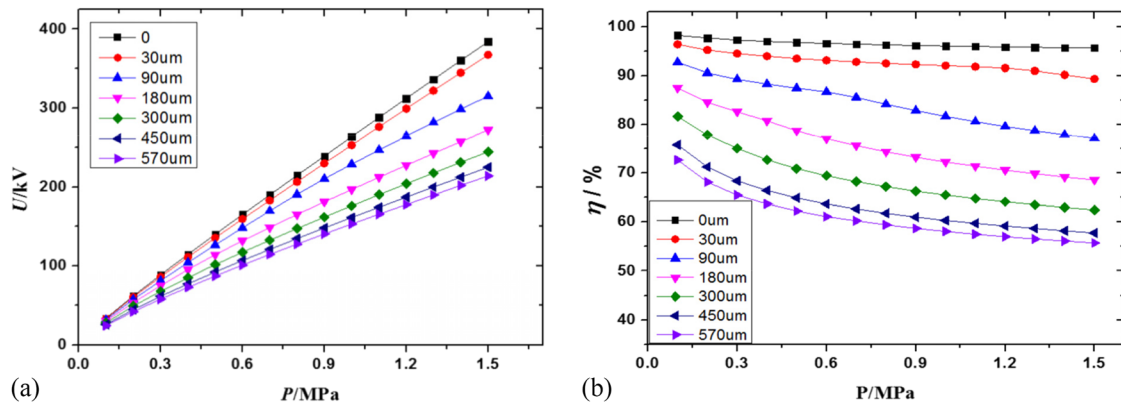


FIG. 4. Calculated U_b - P curves for a 15 mm nitrogen gap. (a) Breakdown voltage vs pressure and (b) percent decline in U_b vs pressure.

avoided by properly decreasing the working coefficient of gas switch.

2. Mode II

When a free microparticle becomes charged (assuming that the potential of the top and bottom electrodes is +HV DC and zero, respectively, and that the microparticle is negatively charged), it departs from the bottom electrode and moves toward the top electrode. Before the microparticle contacts the top electrode, the electric field between the microparticle and top electrode is greatly enhanced, which leads to a microdischarge. At this moment, the microparticle acts as a sharp protrusion on the bottom HV electrode surface and causes a breakdown across the residual gap, as depicted in Fig. 5.²⁵ Although a quantitative calculation of the mode-II breakdown voltage is difficult and prevents a complete analytical analysis, we can say that the field distortion and reduction in the breakdown voltage are much more severe in mode II than those in mode I.

3. Mode III

Multiple particles have a small probability of being generated in the switch gap. Due to random initial conditions, each particle moves randomly under the influence of the electrostatic force and a cascade spatial distribution may occasionally form (see Fig. 6), which significantly enhances the electrical field in the gap and induces voltage breakdown across the gap, as shown in Fig. 6. Although the probability of mode III is

relatively low, it is certain to occur, especially under a DC voltage of relatively long duration. Microparticles in mode III exert a strong influence over the breakdown voltage of the gas switch.

Table I lists the results of tests conducted to determine how microparticles affect the breakdown voltage of an 8 mm air gap at 0.1 MPa, which is similar to the upper gap in Fig. 7. With one or more 300 μm particles in the gap, the breakdown voltage varies. A fixed particle can decrease U_b by 19%, whereas a moving particle can decrease U_b by 24%. When the gap contains more than one particle, a DC voltage is applied for at least 10 min to ensure that multiple particles occupy the most dangerous positions. The results show that, compared with the clean gap, U_b decreases by 33% for two microparticles in the gap and by 43% for three microparticles.

IV. EXPERIMENTAL VERIFICATION OF MECHANISM CAUSING PRE-FIRING

Figure 7 shows a three-electrode field-distortion gas switch, which we use to verify whether microparticles contribute to pre-firing in the switch. The 10-cm-high, 8.5-cm-diameter switch contains two 8 mm gaps and can be pressurized to about 0.8 MPa. The trigger plate is especially designed with a cambered surface to prevent free particles from escaping to regions of a low electric field. Such a design guarantees that the particle remains in the region with a high electric field but does not move to a safe location, thereby greatly improving the

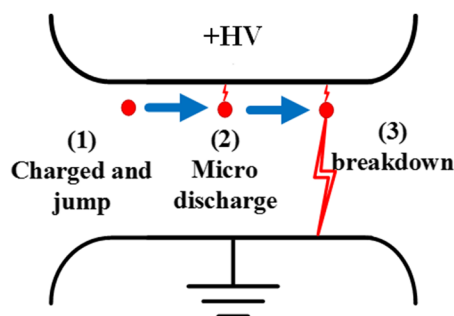


FIG. 5. Mode II: pre-firing induced by a moving microparticle.

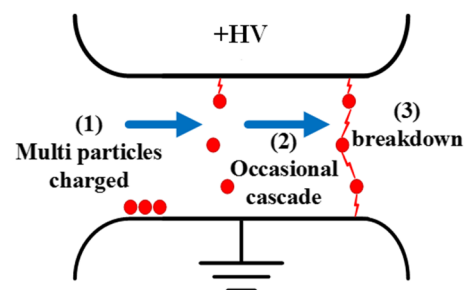


FIG. 6. Mode III: multiple microparticles in the gap.

TABLE I. Breakdown voltage of a gas switch containing microparticles in the gap.

Mode	Clean gap	Mode I (fixed particle)	Mode II (free particle)	Mode III (two particles)	Mode III (three particles)
U_b (kV)	23.2	18.9	17.6	15.5	13.2
$\Delta U/U_b$ (%)	0	19	24	33	43

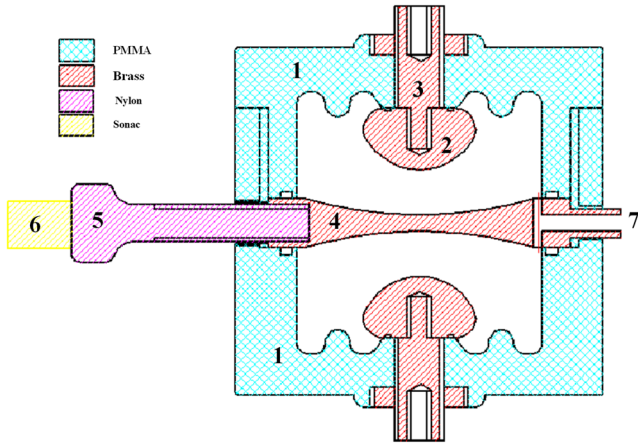


FIG. 7. Structure of three-electrode field-distortion gas switch (1—PMMA shell, 2—main electrode, 3—connection, 4—trigger electrode, 5—insulated connection, 6—ultrasonic probe, 7—gas inlet and outlet).

efficiency of the test without perturbing the other parameters of the switch. In addition, a nylon connection is screwed tightly to the trigger plate to detect the vibration from particle bounce. These signals are monitored using a sensitive ultrasonic probe.

A compact *RLC* discharge called an “LTD brick” which is similar to that used in Ref. 13 is used here to conduct repetitive discharges at triggered mode at a frequency of about 0.02 Hz, while the ultrasonic probe monitors the bounce signals. Table II shows the parameters of the circuit and discharge current. The switch operates at a 75% working coefficient and draws a 30 kA current pulse with a 60 ns rise time with 4.5 mC of charge transferred per pulse.

One pre-firing incident occurred at shot 176, and the monitored waveform is shown in Fig. 8. Note that the bounce signals from microparticles appear in the pre-firing incident, shortly before the collapse of the voltage waveform, whereas only the breakdown signal is detected for the other shots. For shot 176, the ultrasonic signals of microparticle bounce reach about 100 mV, which is clearly distinguishable from the background noise.

This result verifies the existence of microparticles and their influence on pre-firing in FLTD gas switches. Thus, microparticle generation should be inhibited and/or

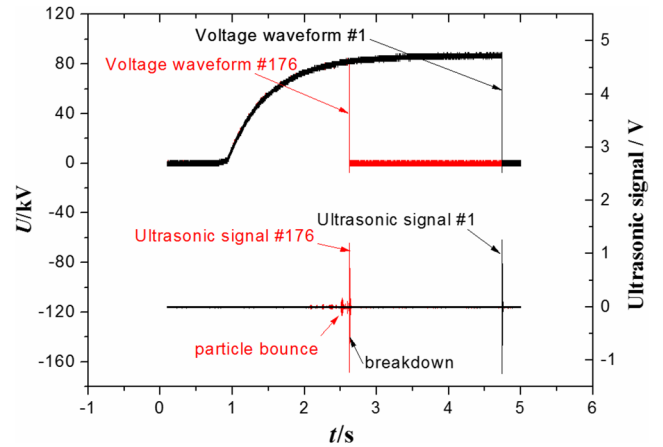


FIG. 8. Ultrasonic signal during repetitive operations of the FLTD gas switch.

microparticle trapping should be improved to minimize the pre-firing probability of gas switches for FLTDs.

V. CONCLUSIONS

This paper presents experimental and theoretical analyses of the behavior of free microparticles to better understand the mechanisms that cause pre-firing in low-inductance gas switches, which have excellent potential for use in FLTDs. The results show that particles are generated during the repetitive discharges of gas switches, including submicrometer powder particles and microparticles ranging in size from tens of micrometers to over 100 μm . Microparticles can be charged and then forced into motion by the electrostatic field in the gap, which significantly decreases the breakdown voltage of gas switches and induces pre-firing. Three different modes of free microparticle motion appear to be responsible for switch pre-firing. (i) Microparticles adhere to the electrode surface and act as a fixed protrusion which distorts the local electric field and initiates the breakdown in the gap. (ii) One particle escapes toward the opposite electrode and causes a near-electrode microdischarge, inducing the breakdown of the residual gap. (iii) Multiple moving microparticles are occasionally in cascade, leading to pre-firing. Experimental results indicate that a 300 μm microparticle fixed on the electrode surface can decrease U_b of an 8 mm nitrogen gap by 19%, while

TABLE II. Parameters of circuit and discharge current.

Parameter	C (nF)	L (nH)	R (Ω)	U (kV)	I (kA)	Q (mC)	t_r (ns)	f (Hz)	γ (%)
Value	20	200	3	± 90	30	4.5	60	0.02	75

a free microparticle can decrease U_b by 24%. Two and three free microparticles can cause a 33% and 43% decrease of U_b , respectively. At last, this microparticle-induced mechanism is experimentally verified in a three-electrode field-distortion gas switch by using a sensitive ultrasonic probe. The ultrasonic signals indicating the “bounce” of microparticles off the electrode surface appear shortly before the collapse of the voltage waveform in pre-firing incidents, which demonstrates the existence of microparticles and their significant contribution to inducing pre-firing in gas switches under the typical working conditions of FLTD.

ACKNOWLEDGMENTS

This work was supported by the National Natural Science Foundation of China under Grant No. 51207127.

- ¹W. Stygar, M. Cuneo, D. Headley, H. Ives, R. Leeper, M. Mazarakis, C. Olson, J. Porter, T. Wagoner, and J. Woodworth, *Phys. Rev. Spec. Top.—Accel. Beams* **10**, 030401 (2007).
- ²D. Ryutov, M. Derzon, and M. Matzen, *Rev. Mod. Phys.* **72**, 167 (2000).
- ³E. Neau, *IEEE Trans. Plasma Sci.* **22**, 2 (1994).
- ⁴J. Wu, M. Li, X. Li, L. Wang, G. Wu, G. Ning, M. Qiu, and A. Qiu, *Phys. Plasma* **20**, 082706 (2013).
- ⁵A. Kim, B. Kovalchuk, E. Kumpyak, and N. Tsoy, *Russ. Phys. J.* **42**, 985 (1999).
- ⁶A. Kim, M. Mazarakis, V. Sinebryukhov, B. Kovalchuk, V. Visir, S. Volkov, F. Baval, A. Bastrikov, V. Durakov, S. Frolov *et al.*, *Phys. Rev. Spec. Top.—Accel. Beams* **12**, 313 (2009).
- ⁷F. Lassalle, A. Loyer, A. Georges, B. Roques, H. Calamy, C. Mangeant, J. Cambonie, S. Laspalles, D. Cadars, G. Rodriguez *et al.*, *IEEE Trans. Plasma Sci.* **36**, 370 (2008).
- ⁸J. Leckbee, J. Maenchen, D. Johnson, S. Portillo, D. Vandevalde, D. Rose, and B. Oliver, *IEEE Trans. Plasma Sci.* **34**, 1888 (2006).
- ⁹C. Boissady and F. Riouxdamidau, *Rev. Sci. Instrum.* **49**, 1537 (1978).
- ¹⁰A. Endoh, S. Watanabe, and M. Watanabe, *J. Appl. Phys.* **55**, 1322 (1984).
- ¹¹Z. Taylor and K. Leopold, *Rev. Sci. Instrum.* **55**, 52 (1984).
- ¹²H. Gundel, H. Riege, J. Handerek, and K. Zioutas, *Appl. Phys. Lett.* **54**, 2071 (1989).
- ¹³J. Woodworth, J. Alexander, F. Gruner, W. Stygar, M. Harden, J. Blickem, G. Dension, F. White, L. Lucero, S. Glover *et al.*, *Phys. Rev. Lett.* **12**, 060401 (2009).
- ¹⁴J. Woodworth, W. Stygar, L. Bennett, M. Mazarakis, H. Anderson, M. Harden, J. Blickem, F. Gruner, and R. White, *Phys. Rev. Lett.* **13**, 080401 (2010).
- ¹⁵W. Tie, S. Liu, X. Liu, Q. Zhang, L. Pang, and L. Liu, *Rev. Sci. Instrum.* **85**, 023504 (2014).
- ¹⁶X. Li, X. Liu, F. Zeng, X. Gou, and Q. Zhang, *IEEE Trans. Plasma Sci.* **43**, 1040 (2015).
- ¹⁷H. Wang, Q. Zhang, X. Tong, X. Liu, and A. Qiu, *Europhys. Lett.* **96**, 45001 (2011).
- ¹⁸X. Li, Z. Pei, Y. Zhang, X. Liu, Y. Li, and Q. Zhang, *Phys. Plasma* **24**, 122108 (2017).
- ¹⁹J. Wu, R. Han, W. Ding, and A. Qiu, *IEEE Trans. Dielectr. Electr. Insul.* **24**, 2164 (2017).
- ²⁰A. Donaldson, *Electrode Erosion in High-Current, High-Energy Transient Arcs* (Texas Tech University, Lubbock, 1991).
- ²¹N. Lebedev and I. Skalskaya, *Sov. Phys. Tech. Phys.* **7**, 268 (1962).
- ²²K. Sakai, D. Abella, Y. Khan, J. Suehiro, and M. Hara, *IEEE Trans. Dielectr. Electr. Insul.* **10**, 404 (2003).
- ²³K. Sakai, D. Abella, Y. Khan, J. Suehiro, and M. Hara, *IEEE Trans. Dielectr. Electr. Insul.* **10**, 418 (2003).
- ²⁴J. Wang, Q. Li, B. Li, C. Chen, S. Liu, and H. Ji, *IEEE Trans. Dielectr. Electr. Insul.* **23**, 2617 (2016).
- ²⁵J. Wang, Q. Li, B. Li, C. Chen, S. Liu, and C. Li, *IEEE Trans. Dielectr. Electr. Insul.* **23**, 1951 (2016).
- ²⁶A. Pederson, *IEEE Trans. Power Appar. Syst.* **PAS-94**, 1749 (1975).
- ²⁷H. Saitoh, K. Morita, T. Kikkawa, N. Hayakawa, and H. Okubo, *IEEE Trans. Dielectr. Electr. Insul.* **9**, 544 (2002).
- ²⁸N. Malik and A. Qureshi, *IEEE Trans. Dielectr. Electr. Insul.* **14**, 70 (1979).